

Porous, rigid metal(III)-carboxylate metal-organic frameworks for the delivery of nitric oxide

Jarrold F. Eubank,^{1,a} Paul S. Wheatley,² Gaëlle Lebars,³ Alistair C. McKinlay,² Hervé Leclerc,³ Patricia Horcajada,¹ Marco Daturi,³ Alexandre Vimont,³ Russell E. Morris,² and Christian Serre¹

¹Institut Lavoisier, UMR CNRS 8180, Université de Versailles Saint-Quentin-en-Yvelines, 45 Avenue des Etats-Unis, 78035 Versailles Cedex, France

²EaStChem School of Chemistry, University of St Andrews, Purdie Building, St Andrews, Fife KY16 9ST, United Kingdom

³Laboratoire Catalyse et Spectrochimie, ENSICAEN, Université de Caen, CNRS; 6, boulevard Maréchal Juin, F-14050 Caen, France

(Received 28 September 2014; accepted 1 December 2014; published online 30 December 2014)

The room temperature sorption properties of the biological gas nitric oxide (NO) have been investigated on the highly porous and rigid iron or chromium carboxylate based metal-organic frameworks Material Institut Lavoisier (MIL)-100(Fe or Cr) and MIL-127(Fe). In all cases, a significant amount of NO is chemisorbed at 298 K with a loading capacity that depends both on the nature of the metal cation, the structure and the presence of additional iron(II) Lewis acid sites. In a second step, the release of NO triggered by wet nitrogen gas has been studied by chemiluminescence and indicates that only a partial release of NO occurs as well as a prolonged delivery at the biological level. Finally, an *in situ* infrared spectroscopy study confirms not only the coordination of NO over the Lewis acid sites and the stronger binding of NO on the additional iron(II) sites, providing further insights over the partial release of NO only in the presence of water at room temperature. © 2014 Author(s). All article content, except where otherwise noted, is licensed under a Creative Commons Attribution 3.0 Unported License. [<http://dx.doi.org/10.1063/1.4904069>]

In the field of functional materials, metal-organic frameworks (MOFs) have emerged as interesting candidates due to practically limitless combinations of organic ligands and inorganic components (single-metal ions, clusters, chains, sheets, etc.), which provides a plethora of inherent functionalities, as well as important porosity, relatively high thermal stability, often mild synthesis conditions, and comprehensive design strategies.¹ The ability to readily design MOFs with particular inbuilt properties or functions has increased scientific interest for their use in targeted applications, and great progress has been made in the areas of gas storage,² carbon capture,³ and fluid separation.⁴ In addition, the biocompatibility of some MOFs has fostered a burgeoning interest in biological applications,⁵ such as the controlled release of drug molecules.⁶ Due to the renowned gas storage abilities of MOFs, attention has also been recently given to the delivery of biologically active gas molecules, especially therapeutics like nitric oxide (NO).⁷

Some of us have recently reported the low toxicity of iron(III) polycarboxylate nanoparticles.⁸ In addition, *a priori* biocompatible MOFs, derived from endogenous cations (i.e., iron and calcium) and/or therapeutic active ligands, have also been synthesized.^{5,9} Some of them have been denoted as BioMILs (Bioactive Materials from Institut Lavoisier),¹⁰ with the ability of the porous nontoxic MOFs to adsorb and release in a controlled manner as demonstrated for a wide range of active molecules.^{5,6} In addition, some of us also reported the ability of porous MOFs that bear Lewis acid sites to uptake and release therapeutic gas molecules, including NO or hydrogen sulfide.⁷ The well-known porous metal(II) dihydroxyterephthalates, denoted CPO-27, are archetype porous MOFs for such biological

^aPresent address: Department of Chemistry and Physics, Florida Southern College, Lakeland, FL 33801, USA.



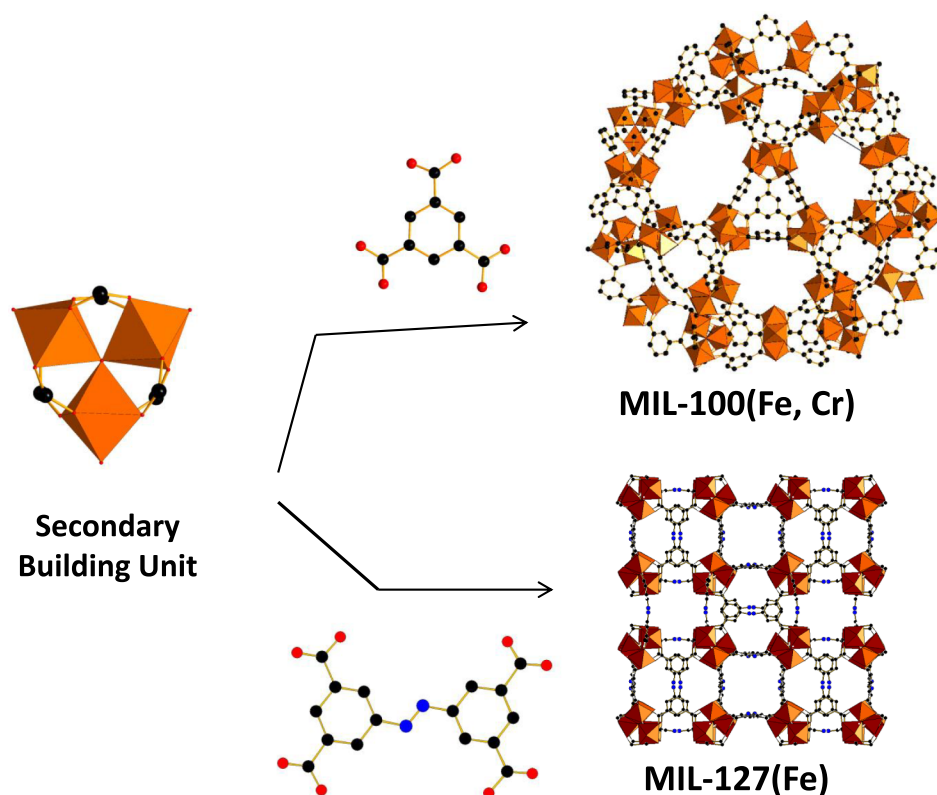


FIG. 1. Representation of the assembly of the rigid, porous, 3-periodic MIL-100(Fe) (top), MIL-127(Fe) (bottom), and MOFs from the inorganic trinuclear iron cluster and tricarboxylate or tetracarboxylate ligands.

gases and their controlled release leading to anti-bacterial and anti-platelet aggregation properties.⁷ More recently, the series of iron(III) dicarboxylates MOFs with MIL-88 architecture (MIL stands for Material Institut Lavoisier),¹¹ composed of linear dicarboxylate organic ligands (e.g., terephthalate) and trinuclear metal clusters ($M_3O(-O_2CR)_6A_3$, ($M = Fe, Cr$; $A =$ solvent molecules or counter-anions) bearing Lewis acid sites, has shown great promise for NO adsorption and delivery,^{7(a)} albeit to a lesser extent than the CPO-27 MOFs,^{7(b),7(c)} due to the lower toxicity ($LD_{50} = 30 \text{ g} \cdot \text{kg}^{-1}$)⁸ and pharmaceutical acceptability of iron based structures.¹²

Though the MIL-88 series offers fine examples of biocompatible and biodegradable iron MOFs suitable for biologically active gas applications, sorption capacities have been shown to be limited due to the flexibility of the frameworks, which lead to relatively narrow pore sizes upon solvent molecules removal.¹¹ To address this issue, we focused our attention to other iron(III)-carboxylate based MOFs (Figure 1) that not only possess the same building units as the MIL-88 series, and thus large amounts of Lewis acid sites, but also rigid frameworks with larger windows/pores, namely, MIL-100(Cr, Fe)¹³ and MIL-127(Fe)¹⁴ (analogous to *sof*-MOF(In)¹⁵). MIL-100 possesses two types of mesoporous cages ($d \sim 24$ and 29 \AA , respectively), accessible through microporous pentagonal and hexagonal windows, while MIL-127(Fe) exhibits a 3D microporous system ($d \sim 5\text{-}7 \text{ \AA}$) with both hydrophobic and hydrophilic features¹⁵ (Figure 1). It has previously been shown that these particular MOFs easily adsorb or separate various types of gas molecules and their ability to coordinate polar or quadrupolar molecules (water, alcohols, C_3 , etc.) has been demonstrated.^{16,17} Such materials have accordingly been evaluated for several applications related to gas sorption, separation,¹⁸ water sorption,^{16(a),18} catalysis,^{13(b),19} and drug delivery,^{5,6,20} among others. Thus, it was expected that these MOFs would more easily adsorb NO molecules on their active metal sites than their MIL-88 counterparts.¹⁶

Here, we report the NO sorption and release properties of a series of porous iron(III) or chromium(III) polycarboxylate MOFs of the MIL-100(Fe or Cr) or $M_3OX[C_6H_3-(CO_2)_3]_2 \cdot xH_2O$ ($M = Fe$ or Cr) and MIL-127(Fe) or $Fe_6O_2X_2[C_{12}N_2H_8-(CO_2)_4]_3 \cdot yH_2O$ structure types ($X =$ anion (F, OH, Cl,

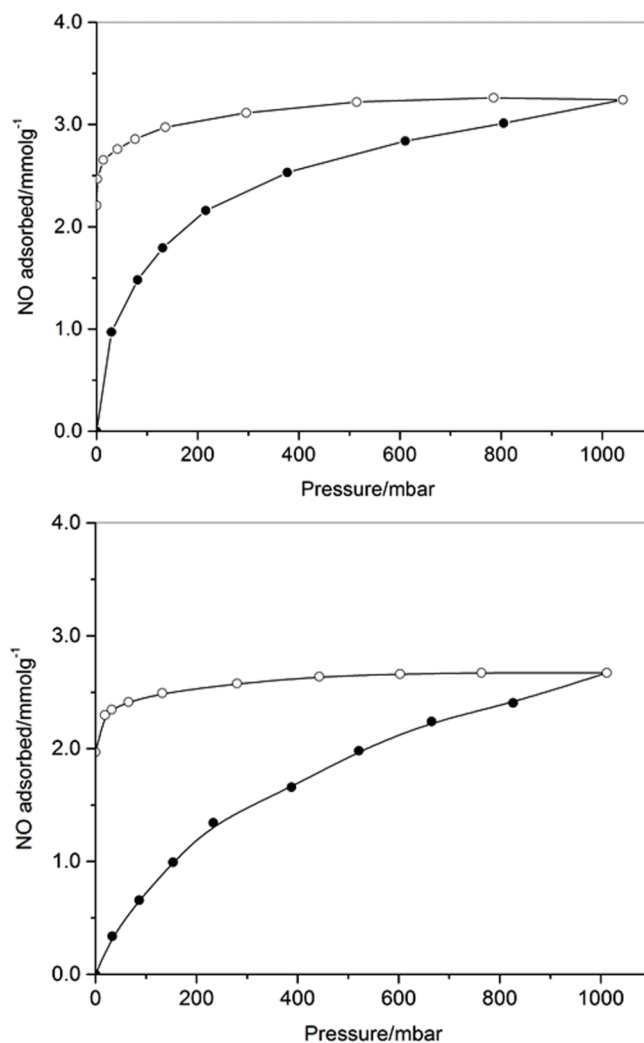


FIG. 2. NO adsorption/desorption isotherms at 298 K of MIL-100(Cr) (top) and MIL-100(Fe) (bottom), respectively, activated at ~ 423 K (adsorption: open symbols; desorption: closed symbols).

etc.); $x \sim 14$, $y \sim 20$). The impact of the thermal activation on the removal of the free water and the coordinated water molecules, particularly for the reducible iron(III) MOFs, whose ability to exhibit additional Fe(II) sites upon partial reduction of iron(III) upon high temperature vacuum treatment has also been assessed.¹⁶ Finally, to gain understanding on the microscopic behavior of these MOFs upon loading or release of NO, *in situ* infrared (IR) spectroscopy experiments have also been carried out.

All of the MOF materials [MIL-100(Cr), MIL-100(Fe), and MIL-127(Fe)] were synthesized according to published procedures.^{13,14} See supplementary material.²¹

In a first step, the NO loading capacity of each of our MOFs of interest, MIL-100(Cr), MIL-100(Fe), and MIL-127(Fe), was assessed through a series of NO sorption experiments (Figure 2, Figure S1, Table I). The samples were heated under primary vacuum at 423 K to remove guest and coordinated solvent molecules. Upon activation, dry NO was introduced, and the adsorption/desorption was monitored over several trials for each material. The adsorption/desorption isotherms of MIL-100(Cr or Fe) are first displayed in Figure 2. As expected from rigid porous MOFs, the isotherms display a type I adsorption, characteristic of microporous materials with a maximum uptake, at 1 bar, within the 2.7–3.2 mmol g^{-1} range, close to the theoretical amount of Lewis acid sites for MIL-100(Fe or Cr) ($\sim 3.6 \text{ mmol g}^{-1}$). In the case of MIL-127 (Figure S1), the amount of adsorbed NO at 1 bar is

TABLE I. Summary of NO adsorption and residual capacity at 298 K for MIL-100(Cr), MIL-100(Fe), and MIL-127(Fe) activated at ~ 523 K (M=Fe).

Solid	Average adsorption capacity (mmol g^{-1})	Residual capacity upon desorption (mmol g^{-1})
MIL-100(Cr)	3.3(2)	2.5(2)
MIL-100(Fe ^{III})	2.7(2)	2.0(2)
MIL-100(Fe ^{II/III})	4.5(3)	3.2(2)
MIL-127(Fe ^{III})	1.2(2)	0.75(10)
MIL-127(Fe ^{II/III})	2.2(2)	1.4(2)

much smaller, close to $1.2(2) \text{ mmol g}^{-1}$, less than half of the theoretical value ($\sim 2.7 \text{ mmol g}^{-1}$). In the case of the MIL-88A and MIL-88B flexible materials, a slightly lower amount of experimental adsorbed NO was previously obtained (range of $1\text{-}2.5 \text{ mmol g}^{-1}$) compared to the theoretical values ($2.5\text{-}4 \text{ mmol g}^{-1}$), which was attributed to the presence of the very narrow pores of their dried forms, limiting thus the accessibility of the metal sites to NO. In the case of MIL-127, one can assume that the narrow pores ($\sim 5\text{-}7 \text{ \AA}$) are here not fully accessible to NO due to the presence of a significant

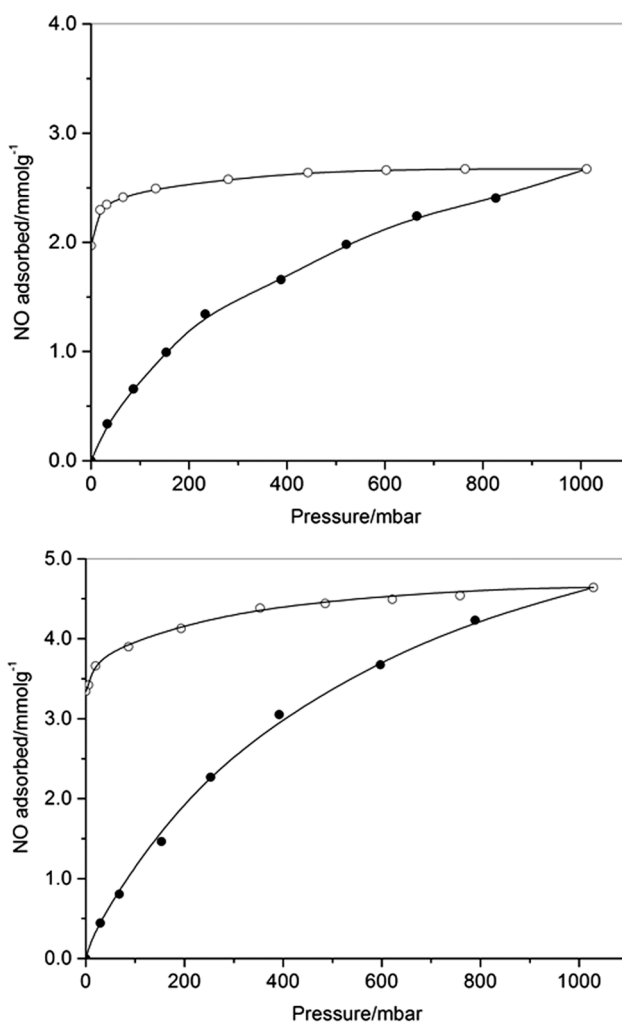


FIG. 3. Comparison of the NO adsorption/desorption isotherms at 298 K of MIL-100(Fe) after activation at ~ 423 K (top) and 523 K (bottom), respectively. (adsorption: open symbols; desorption: closed symbols).

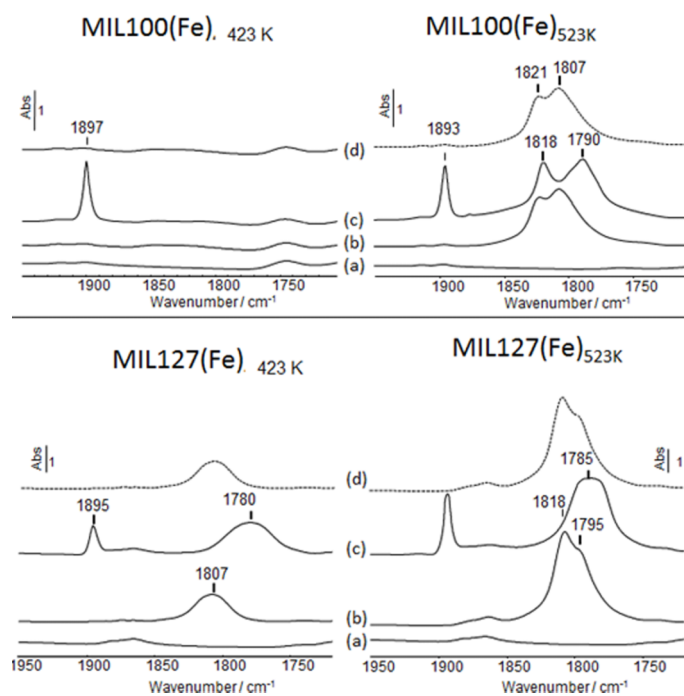


FIG. 4. IR spectra of MIL-100(Fe) (upper part) and MIL-127(Fe) (lower part) activated at 423 K (left) or 523 K (right) (spectra (a)). IR spectra of NO ($P_{\text{NO}} = 25$ millibars) adsorbed at 298 K (b), at 220 K (c), and then after outgassing at 298 K (spectra (d), dotted line).

amount of remaining coordinated water molecules after activation at 423 K only, as observed previously for MIL-100(Fe or Cr), preventing from the full accessibility of the open metal sites within the micropores. For MIL-100, the impact is less pronounced due to the much larger pore size. As in the case of other rigid MOFs (CPO-27s, HKUST-1, etc.),^{7(b)} a pronounced hysteresis is observed in each case for the desorption branch, in agreement with part of the NO being retained on the Lewis acid sites at very low pressure.

In a second step, keeping in mind that upon activation at higher temperatures under vacuum (~ 523 K), it was previously shown that the iron(III)-carboxylate MOFs based on the oxo-centered trimeric sub-units (MIL-100, MIL-88s) could undergo a partial reduction of iron(III) into iron(II),^{7(a),16(b),20} leading to additional accessible Fe(II) sites thus available for a stronger interaction through back donating effect with unsaturated guest molecules. We decided to study the impact of the temperature of activation of the iron MOFs on NO sorption.

After activation of MIL-100(Fe) or MIL-127(Fe) at 523 K, we observe, in both cases, a significant increase in the total amount of adsorbed NO (Figure 3, Figure S1), up to $4.5(3)$ mmol g^{-1} in MIL-100(Fe), with nearly of $3.2(2)$ mmol g^{-1} remaining upon desorption. In the case of MIL-127(Fe), the same effect occurs (Figure S1) with the uptake going from $1.2(2)$ to $2.2(2)$ mmol g^{-1} . These results confirm that both NO sorption capacity and affinity increase upon the occurrence of additional Fe(II) metal sites forming upon under vacuum during the activation process.

Such an increase of the NO capacity and affinity is, on the whole, supported by *in situ* IR data. The infrared spectra of MIL-100(Fe) and MIL-127(Fe) recorded after NO adsorption (Figure 4) display a strong doublet of bands around 1800 cm^{-1} , assigned to NO adsorbed on Fe(II) coordinatively unsaturated sites (CUS).²⁰ These bands are much stronger after activation at 523 K, whereas the band of NO adsorbed on Fe(III) metal sites, observed at 1895 – 1900 cm^{-1} , remains almost constant for MIL-100(Fe), and only slightly increases for MIL-127(Fe). This confirms that, upon higher activation temperatures, supplementary Fe(II) metal sites become able to interact with NO in both cases. In fact, these Fe^{II}-NO sites appear to be more stable at higher temperatures (e.g., room temperature (298 K), Figs. 4(b) and 4(d)), due to the back donation effect,^{16(b),20} which partly explains why the affinity of these iron-carboxylate based MOFs toward NO increases upon thermal treatment.

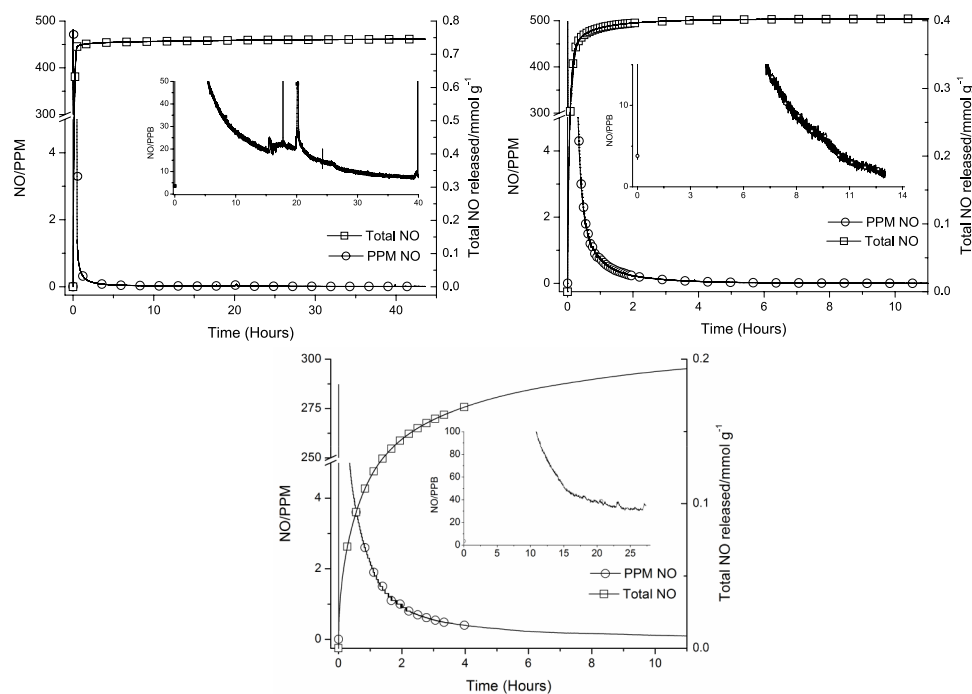


FIG. 5. Example of NO desorption from MIL-100(Cr), MIL-100(Fe), and MIL-127(Fe) activated at 423 K overnight, respectively. Insets are in parts per billion range.

In order to probe the interest of the NO loaded samples, we performed a series of NO release experiments. The release of NO was triggered from MIL-100(Cr), MIL-100(Fe), and MIL-127(Fe) by passing humid nitrogen gas (11% relative humidity and 200 ml min⁻¹ R.H.) over the NO-loaded samples and quantified by chemiluminescence. The results are shown in Figure 5 (and Figures S2–S6) and summarized in Table II. MIL-100(Cr) released the largest amount of NO, as well as the largest relative amount of NO compared to MIL-100(Fe) followed by MIL-127(Fe). In the case of MIL-127(Fe) activated at higher temperatures, the impact of the presence of additional Fe(II) sites was confirmed, as evidenced by an increase in the amount of desorbed NO from ~0.18 to ~0.49 mmol g⁻¹, due to the stronger ability of Fe(II) sites to retain NO upon desorption under vacuum. The same effect is on the whole observed for MIL-100(Fe) whose partial reduction also increases by ca. 50% the overall amount of desorbed NO (see supplementary material). This is in agreement with the stronger interaction strength of Fe(II) sites compared with the Fe(III) ones.

Once again, whatever the nature of the cation (Cr or Fe) or the structure, as previously reported for the iron-dicarboxylate MIL-88 solids,^{7(a)} only part of the adsorbed NO is released in the presence of moisture, i.e., around 20% of the initial chemisorbed NO. As reported previously, this might be due to a partial release of NO over the weakest metal sites (i.e., Fe(III)) between the loading and release tests.^{7(a)} This value is, however, except for the pure iron(III) MIL-127, slightly larger than in

TABLE II. Summary of NO adsorption capacity and released NO.

Adsorbent	Residual desorption capacity (mmol g ⁻¹)	Released NO (mmol g ⁻¹)	% NO released ^a
MIL-100(Cr)	2.5(2)	0.65	26
MIL-100(Fe ^{III})	2.0(2)	0.35	15
MIL-100(Fe ^{II/III})	3.2(2)	0.55	17
MIL-127(Fe ^{III})	0.75(10)	0.2	27
MIL-127(Fe ^{II/III})	1.4(1)	0.5	36

^aPercentage calculated from the initial amount adsorbed at 1 bar.

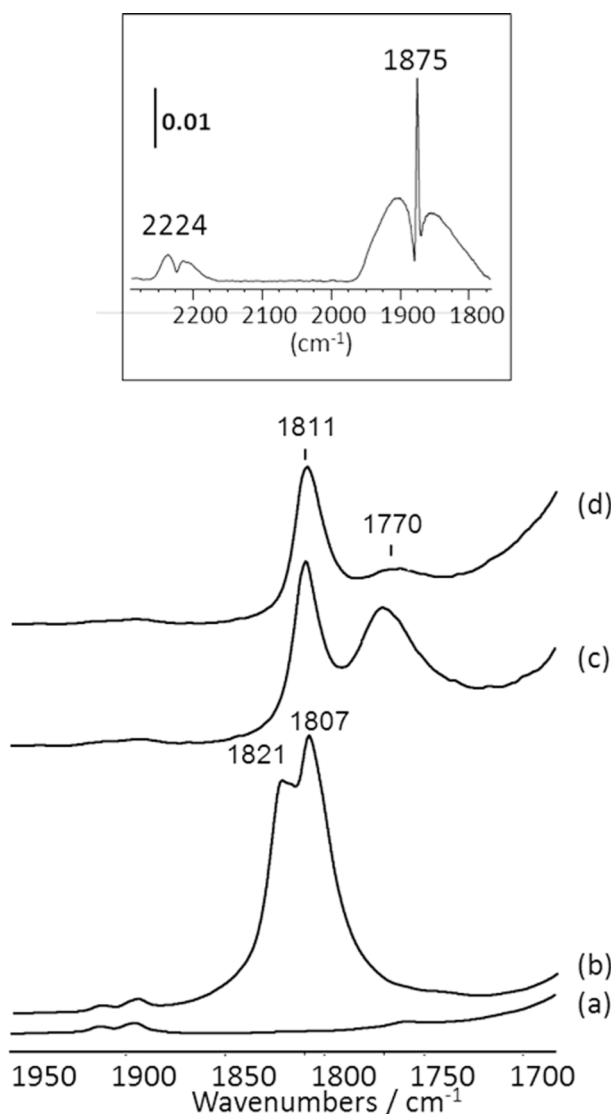


FIG. 6. Infrared spectra of MIL-100(Fe) activated at 523 K (a), followed by introduction of NO and evacuation under vacuum at 298 K (b), and a subsequent introduction of an equilibrium pressure of water vapor into the cell (~ 12 millibars) (spectra (c) and (d) are recorded after 1 min and 7 h of water exposure, respectively). Inset: gas phase spectrum recorded after 7 h (contribution of water to the spectrum has been subtracted).

the case of the flexible solid analogues ($< 0.3 \text{ mmol g}^{-1}$), but still far the initial adsorbed amounts ($2\text{--}4 \text{ mmol g}^{-1}$). Upon partial reduction, we observe a significant increase in the overall release of NO probably due to the presence of the Fe(II) sites able to interact strongly with NO through back donation effect.²⁰ As for the MIL-88 materials, the rather low amount of released NO might here be partially due to a significant desorption of NO under vacuum prior to the release tests.

The benefits of NO as a biological gas are numerous, and the encapsulation with porous materials is of scientific interest. The NO-loaded MOFs are of interest due to their high content of chemisorbed NO which could be used either as (i) an antibacterial agent that can be released during the first step of the moisture-triggered release or (ii) an antithrombotic agent when released slowly at the biological level (threshold of ~ 10 ppb of released NO per minute).⁷ If in the present case, as for the flexible MIL-88 solids,^{7(a)} the interest of the porous iron MOFs might not be that significant for the antibacterial effect due to the rather low released amounts, the situation is different for the slow release at the biological level. If the best MOF seems here at first sight, the MIL-100(Cr) solid with a rather

long release up to 40 h, as expected from its higher Lewis acidic character,²² the chromium toxicity might hamper its practical use. In contrast, the biocompatible MIL-100(Fe) exhibits, on the whole, a controlled release at the biological level of ~7 h (non reduced) (Figure 5) or ~20 h (partially reduced) (Figure S4). The MIL-127(Fe) MOFs exhibits a better release at the biological level than MIL-100 of at least 25 h, the released value at 25 h being still higher than the biological threshold. This makes these iron based MOFs potential candidates for NO release. Note here the positive impact of the additional iron(II) sites that strongly enhances for both MIL-100 and MIL-127 the release times at the biological level. Concerning the porous rigid iron carboxylate MOFs of the present study, the kinetics of release is on the whole superior, in terms of prolonged release at the biological level, to the one observed previously for the flexible MIL-88s^{7(a)} and that of the porous bioactive calcium-tetracarboxylate MOF, BioMIL-4.^{10(a)}

To better understand the mechanism of NO release in presence of moisture, we have introduced water vapor on MIL-100(Fe)_{523 K} (i.e., activated at 523 K) that was first exposed to NO at 298 K and then outgassed under secondary vacuum. As mentioned above, upon exposure to NO at room temperature, peaks appear at 1822 cm⁻¹ and 1807 cm⁻¹ (Figure 6(b)), due to Fe^{II} (NO) formation.

The presence of two bands reveals the presence of two different Fe^{II} sites. Introduction of water into the cell immediately downward shifts the 1807 cm⁻¹ ν (NO) component to 1770 cm⁻¹ whereas the 1821 cm⁻¹ component is much less affected: it shifts to 1811 cm⁻¹ without any significant change in intensity (Fig. 4(c)). Spectra recorded after 7 h under water pressure show that the 1770 cm⁻¹ band intensity strongly decreases whereas the intensity of the 1811 cm⁻¹ component slightly decreases. The presence of NO in the gas phase (ν NO band at 1875 cm⁻¹, Fig. 4 inset) and the decrease of the intensity of the adsorbed nitrosyl band in presence of water reveals a competitive adsorption process of H₂O and NO mainly on Fe^{II} sites, characterized by the band at 1807 cm⁻¹ (dry sample) or 1770 cm⁻¹ (hydrated sample). It is also noted the presence of a small amount of N₂O in the gas phase, probably resulting from a slight NO reactivity in presence of water. In this sense, some of us reported very recently that at room temperature, the unexpected ability of porous iron carboxylate MIL-100(Fe) or MIL-127(Fe) to catalytically dissociate NO_x.²³ This could have additional reasons to explain the lower release of NO from these porous iron-carboxylate MOFs compared to the CPO-27 metal(II) based MOFs.

The biologically active NO gas sorption and release on the porous rigid iron(II, III)- or chromium(III)-polycarboxylates based MOFs, MIL-100(Fe, Cr) and MIL-127(Fe), have been evaluated through a combination of adsorption/desorption experiments, chemiluminescence release tests, and *in situ* infra-red spectroscopic analysis. In all cases, it appears that the Lewis acid sites of these MOFs are able to chemisorb a few mmol g⁻¹ of NO at 298 K, with an impact of both the Lewis acidic characters (Cr^{III} > Fe^{III}) or the reducibility of the metal sites (Fe^{II} > Fe^{III}) upon higher temperature activation. It has also been evidenced that only part of the initially chemisorbed NO is released during the chemiluminescence experiments, typically 20%, with an increase of the total amount when Fe^{II} sites are introduced in the MOF. In all cases, an interesting slow release at the biologically antithrombogenic level over a prolonged period of time is observed particularly when iron(II) sites are available. IR spectroscopy confirmed the chemisorption of NO over the iron(II and III) sites with a much better stability of the Fe^{II}:NO interactions at room temperature. It also showed that among the two different Fe^{II}:NO sites detected from IR experiments, only one of them was clearly sensitive to the presence of water at 298 K leading to a partial release of the NO coordinated to the Fe^{II} sites. Further spectroscopic experiments are under progress in order to understand the complex behavior of NO-loaded (reducible) iron MOFs.

This work was supported by CNRS, EU through the ERC-2007-209241-BioMOFs ERC grant (J.F.E., P.H., C.S.). R.E.M. thanks the GEMI Fund and the E.P.S.R.C for funding. R.E.M is a Royal Society Wolfson Merit Award Holder.

¹ (a) Q.-L. Zhua and Q. Xu, "Themed issue: Metal-organic frameworks," *Chem. Soc. Rev.* **43**(16), 5468 (2014); (b) G. Férey, "Hybrid porous solids: Past present future," *ibid.* **37**, 191 (2008).

² J. Sculley, D. Yuan, and H.-C. Zhou, "The current status of hydrogen storage in metal-organic frameworks—Updated," *Energy Environ. Sci.* **4**, 2721 (2011).

³ K. Sumida, D. L. Rogov, J. A. Mason, T. M. McDonald, E. D. Bloch, Z. R. Herm, T.-H. Bae, and J. R. Long, "Carbon dioxide capture in metal-organic frameworks," *Chem. Rev.* **112**(2), 724 (2012).

- ⁴ J.-R. Li, R. J. Kuppler, and H.-C. Zhou, "Selective gas adsorption and separation in metal-organic frameworks," *Chem. Soc. Rev.* **38**, 1477 (2009).
- ⁵ P. Horcajada, R. Gref, T. Baati, P. K. Allan, G. Maurin, P. Couvreur, G. Férey, R. E. Morris, and C. Serre, "Metal-organic frameworks in biomedicine," *Chem. Rev.* **112**, 1232 (2010).
- ⁶ V. Agostoni, T. Chalati, P. Horcajada, H. Willaime, R. H. Anand, T. Baati, S. Hall, G. Maurin, H. Chacun, K. Buchemal, C. Martineau, F. Taulelle, P. Couvreur, C. Roger-Kreuz, P. Clayette, S. Monti, C. Serre, and R. Gref, *Adv. Healthcare Mater.* **2**(12), 1630-1637 (2013); P. Horcajada, T. Chalati, C. Serre, B. Gillet, C. Sebrie, T. Baati, J. F. Eubank, E. Heurtaux, P. Clayette, C. Kreuz, J.-S. Chang, Y. K. Hwang, V. Marsaud, P.-N. Bories, L. Cynober, S. Gil, G. Férey, P. Couvreur, and R. Gref, "Porous metal-organic-framework nanoscale carriers as a potential platform for drug delivery and imaging," *Nat. Mater.* **9**, 172 (2010); R. Ananthoji, J. F. Eubank, F. Nouar, H. Mouttaki, M. Eddaoudi, and J. P. Harmon, "Symbiosis of zeolite-like metal-organic frameworks (*rho*-ZMOF) and hydrogels: Composites for controlled drug release," *J. Mater. Chem.* **21**, 9587 (2011); M. L. K. Taylor-Pashow, J. D. Rocca, Z. Xie, S. Tran, and W. Lin, "Post-synthetic modifications of iron-carboxylate nanoscale metal-organic frameworks for imaging and drug delivery," *J. Am. Chem. Soc.* **131**(40), 14261 (2009).
- ⁷ (a) A. C. Mckinlay, J. F. Eubank, S. Wuttke, B. Xiao, P. S. Wheatley, P. Bazin, J.-C. Lavalley, M. Daturi, A. Vimont, G. De Weireld, P. Horcajada, C. Serre, and R. E. Morris, "Nitric oxide adsorption and delivery in flexible MIL-88(Fe) metal-organic frameworks," *Chem. Mater.* **25**(9), 1592 (2013); (b) N. J. Hinks, A. C. Mckinlay, B. Xiao, P. S. Wheatley, and R. E. Morris, "Metal organic frameworks as NO delivery materials for biological applications," *Microporous Mesoporous Mater.* **129**(3), 330 (2010); (c) A. C. Mckinlay, B. Xiao, D. S. Wragg, P. S. Wheatley, I. L. Megson, and R. E. Morris, "Exceptional behavior over the whole adsorption-storage-delivery cycle for NO in porous metal organic frameworks," *J. Am. Chem. Soc.* **130**(31), 10440 (2008); (d) P. K. Allan, P. S. Wheatley, D. Aldous, M. I. Mohideen, C. Tang, J. A. Hriljac, I. L. Megson, K. W. Chapman, G. de Weireld, S. Vaesen, and R. E. Morris, "Metal-organic frameworks for the storage and delivery of biologically active hydrogen sulfide," *Dalton Trans.* **41**(14), 4060 (2012).
- ⁸ T. Baati, L. Njim, F. Neffati, A. Kerkeni, M. Bouttemi, R. Gref, M. F. Najjar, A. Zakhama, P. Couvreur, C. Serre, and P. Horcajada, "In depth analysis of the in vivo toxicity of nanoparticles of porous iron(III) metal-organic frameworks," *Chem. Sci.* **4**, 1597 (2013); C. Tamames-Tabar, D. Cunha, E. Imbulzqueta, F. Ragon, C. Serre, M. J. Blanco-Prieto, and P. Horcajada, "Cytotoxicity of nanoscaled metal-organic frameworks," *J. Mater. Chem. B* **2**, 262-271 (2014).
- ⁹ (a) I. Imaz, M. Rubio-Martinez, J. An, I. Sole-Font, N. L. Rosi, and D. Maspoeh, "Metal-biomolecule frameworks (MBioFs)," *Chem. Commun.* **47**, 7287 (2011); (b) J. Rabone, Y.-F. Yue, S. Y. Chong, K. C. Stylianou, J. Bacsá, D. Bradshaw, G. R. Darling, N. G. Berry, Y. Z. Khimiyak, A. Y. Ganin, P. Wiper, J. B. Claridge, and M. J. Rosseinsky, "An adaptable peptide-based porous material," *Science* **329**, 1053 (2010); (c) R. Anedda, D. V. Soldatov, I. L. Moudrakovski, M. Casu, and J. A. Ripmeester, "A new approach to characterizing sorption in materials with flexible micropores," *Chem. Mater.* **20**, 2908 (2008); (d) H. Y. Lee, J. W. Kampf, K. S. Park, and E. N. G. Marsh, "Covalent metal-peptide framework compounds that extend in one and two dimensions," *Cryst. Growth Des.* **8**, 296 (2008); (e) M. Tiliakos, E. Katsoulakou, A. Terzis, C. Raptopoulou, P. Coropatis, and E. Manessi-Zoupa, "The dipeptide H-Aib-l-Ala-OH ligand in copper(II) chemistry: Variation of product identity as a function of pH," *Inorg. Chem. Commun.* **8**, 1085 (2005); (f) C. Serre, F. Millange, S. Surblé, and G. Férey, "A route to the synthesis of trivalent transition-metal porous carboxylates with trimeric secondary building units," *Angew. Chem., Int. Ed.* **43**(46), 6285 (2004).
- ¹⁰ (a) S. R. Miller, E. Alvarez, L. Fradcourt, T. Devic, S. Wuttke, P. S. Wheatley, N. Steunou, C. Bonhomme, C. Gervais, D. Laurencin, R. E. Morris, A. Vimont, M. Daturi, P. Horcajada, and C. Serre, "A rare example of a porous Ca-MOF for the controlled release of biologically active NO," *Chem. Commun.* **49**, 7773 (2013); (b) S. R. Miller, P. Horcajada, and C. Serre, "Small chemical causes drastic structural effects: The case of calcium glutarate," *CrystEngComm* **13**, 1894 (2011); (c) S. R. Miller, D. Heurtaux, T. Baati, P. Horcajada, J.-M. Grenèche, and C. Serre, "Biodegradable therapeutic MOFs for the delivery of bioactive molecules," *Chem. Commun.* **2010**, 4526
- ¹¹ C. Serre, C. Mellot-Draznieks, S. Surblé, N. Audebrand, Y. Fillinchuk, and G. Férey, "The role of solvent-host interactions that lead to very large swelling of hybrid frameworks," *Science* **315**, 1828 (2007).
- ¹² (a) S. F. Clark, "Iron deficiency anemia," *Nutr. Clin. Pract.* **23**, 128 (2008); (b) A. Besarab and D. W. Coyne, "Iron supplementation to treat anemia in patients with chronic kidney disease," *Nat. Rev. Nephrol.* **6**, 699 (2010); (c) J. S. Franzone, M. C. Reboani, U. Mason, and F. Villani, "Synthesis of a new anti-anaemic iron lysozyme glutarate complex and pharmacological studies in animals," *Arzneimittelforschung* **40**(9), 987 (1990).
- ¹³ (a) G. Férey, C. Serre, C. Mellot-Draznieks, F. Millange, S. Surblé, J. Dutour, and I. Margiolaki, "Access to a giant pores hybrid solid (>380 000 Å³) by combination of mastered chemistry, simulation and powder diffraction," *Angew. Chem., Int. Ed.* **43**, 6296 (2004); (b) P. Horcajada, S. Surblé, C. Serre, D.-Y. Hong, Y.-K. Seo, J. S. Chang, J.-M. Grenèche, I. Margiolaki, and G. Férey, "Synthesis and catalytic properties of MIL-100(Fe), an iron(III) carboxylate with large pores," *Chem. Commun.* **2007**, 2820
- ¹⁴ D. Cunha, M. B. Yahia, S. Hall, S. R. Miller, H. Chevreau, E. Elkaïm, G. Maurin, P. Horcajada, and C. Serre, "Rationale of drug encapsulation and release from biocompatible porous metal-organic frameworks," *Chem. Mater.* **25**(14), 2767 (2013).
- ¹⁵ Y. Liu, J. F. Eubank, A. J. Cairns, J. Eckert, V. C. Kravtsov, R. Luebke, and M. Eddaoudi, "Assembly of metal-organic frameworks (MOFs) based on indium-trimer building blocks: A porous MOF with *soc* topology and high hydrogen storage," *Angew. Chem., Int. Ed.* **46**, 3278 (2007).
- ¹⁶ (a) Y.-K. Seo, J. W. Yoon, J. S. Lee, Y. K. Hwang, C. H. Jun, J.-S. Chang, S. Wuttke, P. Bazin, A. Vimont, M. Daturi, S. Bourrelly, P. L. Llewellyn, P. Horcajada, C. Serre, and G. Férey, "Energy-efficient dehumidification over hierarchically porous metal-organic frameworks as advanced water adsorbents," *Adv. Mater.* **24**, 806 (2012); (b) H. Leclerc, A. Vimont, J. C. Lavalley, M. Daturi, A. D. Wiersum, P. L. Llewellyn, P. Horcajada, G. Férey, and C. Serre, "Infrared study of the influence of reducible iron(III) metal sites on the adsorption of CO, CO₂, propane, propene and propyne in the mesoporous metal-organic framework MIL-100," *Phys. Chem. Chem. Phys.* **13**(24), 11748 (2011).
- ¹⁷ (a) M. G. Plaza, A. M. Ribeiro, A. Ferreira, J. C. Santos, Y. K. Hwang, Y.-K. Seo, U.-H. Lee, J.-S. Chang, J. M. Loureiro, and A. E. Rodrigues, "Separation of C3/C4 hydrocarbon mixtures by adsorption using a mesoporous iron MOF: MIL-100(Fe),"

- Microporous Mesoporous Mater.* **153**, 178 (2012); (b) J. W. Yoon, Y.-K. Seo, Y. K. Hwang, J.-S. Chang, H. Leclerc, S. Wuttke, P. Bazin, A. Vimont, M. Daturi, E. Bloch, P. L. Llewellyn, C. Serre, P. Horcajada, J.-M. Grenèche, A. E. Rodrigues, and G. Férey, "Controlled reducibility of a metal–organic framework with coordinatively unsaturated sites for preferential gas sorption," *Angew. Chem., Int. Ed.* **49**, 5949–5952 (2010).
- ¹⁸ A. Dhakshinamoorthy, M. Alvaro, P. Horcajada, E. Gibson, M. Vishnuvarthan, A. Vimont, J.-M. Grenèche, C. Serre, M. Daturi, and H. Garcia, "Comparison of porous iron trimesates basolite F300 and MIL-100(Fe) as heterogeneous catalysts for Lewis acid and oxidation reactions: Roles of structural defects and stability," *ACS Catal.* **2**(10), 2060 (2012).
- ¹⁹ R. C. Huxford, J. Della Rocca, and W. Lin, "Metal-organic frameworks as potential drug carriers," *Curr. Opin. Chem. Biol.* **14**(2), 262 (2010).
- ²⁰ S. Wuttke, P. Bazin, A. Vimont, C. Serre, Y. Seo, Y. K. Hwang, J. S. Chang, G. Férey, and M. Daturi, "Discovering the active sites for C3 separation in MIL-100(Fe) by using operando IR spectroscopy," *Chemistry* **18**(38), 11959 (2012).
- ²¹ See supplementary material at <http://dx.doi.org/10.1063/1.4904069> for thermal analysis, NO loading, sorption, release, XRPD, and IR data.
- ²² B. Van de Voorde, M. Boulhout, F. Vermoortele, P. Horcajada, D. Cunha, J. S. Lee, J.-S. Chang, E. Gibson, M. Daturi, J.-C. Lavalley, A. Vimont, I. Beurroies, and D. E. De Vos, "N/S-heterocyclic contaminant removal from fuels by the mesoporous metal–organic framework MIL-100: The role of the metal ion," *J. Am. Chem. Soc.* **135**(26), 9849 (2013).
- ²³ M. Daturi, J. S. Chang, C. Serre, P. Horcajada-Cortes, G. Férey, A. Vimont, Y. K. Hwang, and J. W. Yoon, "Utilisation d'un solide hybride cristallin poreux comme catalyseur de réduction d'oxydes d'azote et dispositifs" International patent FR2010000402, 28 May 2009.

